THE ASTROPHYSICAL JOURNAL, 331:467–476, 1988 August 1

A SPECTRAL DISSECTION OF THE ULTRAVIOLET EMISSIONS OF CAPELLA

THOMAS R. AYRES[1]
Center for Astrophysics and Space Astronomy, University of Colorado
Received 1987 September 3; accepted 1988 January 19

ABSTRACT

Phase-resolved observations of Capella (α Aurigae A: G5 III + G0 III) were conducted with the *International Ultraviolet Explorer* (*IUE*) in order to separate the spectrum of the core-helium-burning (CHeB) primary (Aa) from that of the fast-rotating, chromospherically active secondary (Ab).

The emission lines of the primary were isolated by modeling the residuals formed by subtracting spectra, from radial velocity extrema, in the frame of reference of the secondary. Spectra from several orbital phases then were corrected for the small contributions by the primary, and averaged to yield high-quality line shapes for the secondary.

The ultraviolet emissions of the primary were compared to those of the four K0 giants of the Hyades, and the field K giants β Cet and β Gem. In terms of C IV ($\approx 10^5$ K) emission, the six reference CHeB giants fall into two distinct groups: the more active β Cet type; and the less active β Gem type. The two prototypes also show quantitatively different behavior in their chromospheric He I λ10830 absorption. In terms of its C IV flux and large λ10830 equivalent width, Capella Aa clearly belongs in the β Cet group.

The similarity between the Capella primary and the two active Hyads—γ Tauri and θ^1 Tauri—is striking, particularly in light of the possible association of Capella with the young open cluster on the basis of space motion. Indeed, if Capella truly is coeval with the Hyades nucleus, then the age of the cluster might be less than *half* that commonly assumed.

Furthermore, if the primary is a recent addition to the CHeB "clump," the dramatic decline in average rotation rates from spectral type ~G0 to G9–K0 likely occurs in two distinct stages: (1) a rapid phase during the first crossing through the Hertzsprung gap, governed by internal redistribution of angular momentum; and (2) a gradual phase in the clump, governed by the torquing of a weak stellar wind.

The pristine spectra of the Capella secondary reveal asymmetries at the peaks of several of the high-excitation features, particularly C II λ1335 and C IV λ1548. That in the optically thick C II emission is suggestive of mass *outflow* at the $\sim 2 \times 10^4$ K level of the upper chromosphere, although the flow very likely is part of a *circulation system* like that thought to operate in magnetic active regions on the Sun. *Redshifts* of the optically thin lines of high excitation—Si III] λ1892 and C III] λ1908—possibly reveal the reverse leg of the circulation system. However, the lack of a significant Doppler shift in C IV λ1548, but the existence of a significant redshift in the other member of the doublet (λ1550), is puzzling: λ1548 might be optically thick enough that a "reverse P Cygni" effect masks an intrinsic redshift; however, other phenomena (like blends) cannot be ruled out at present. Finally, the behavior of Cl I λ1351 supports Shine's proposal that it is radiatively pumped by C II λ1335.

Subject headings: clusters: open — stars: binaries — stars: individual (α Aur) — stars: late-type — ultraviolet: spectra

I. INTRODUCTION

Capella (α Aurigae A: G5 III [Aa] + G0 III [Ab]; HD 34029: Hoffleit and Jaschek 1982) has been the focus of numerous studies ranging broadly over the electromagnetic spectrum: optical spectroscopy of it has continued unabated since the turn of the century (see, e.g., Griffin and Griffin 1986, and references therein); it was one of the first targets of vacuum-ultraviolet and X-ray instruments in the modern era of sounding rockets and satellites (e.g., Dupree 1975; Vitz *et al.* 1976; Cash *et al.* 1978; Ayres and Linsky 1980; Mewe *et al.* 1982); and it is one of the few late-type objects detected in centimeter radio waves (Drake and Linsky 1986).

The popularity of the 104 day binary stems partly from its large apparent brightness at all of these wavelengths. Furthermore, Capella consists of a pair of rare "yellow giants" (spectral type F or G): such stars often exhibit substantial fluxes of C IV (~10^5 K) and soft X-rays (≳10^6 K) despite the very low levels, or absence, of such emissions among the more common red giants (spectral types K and M) (e.g., Ayres *et al.* 1981).

A third compelling reason to study the nearby (13.2 pc) binary is that it is a member of the Hyades moving group by virtue of its space motion (Eggen 1960). Accordingly, the yellow giants of Capella are appropriate candidates for comparative studies with respect to the four, more evolved ~K0 giants in the nuclear region of the cluster (cf. Baliunas, Hartmann, and Dupree 1983).

Early observations of Capella with the *International Ultraviolet Explorer* (*IUE*) by Ayres and Linsky (1980) revealed that most of the high-excitation, ultraviolet flux arises in the outer atmosphere of the fast-rotating secondary ($v \sin i_{Ab} \approx 36$ km s^{-1}) rather than the somewhat more massive, cooler, and more slowly rotating primary ($v \sin i_{Aa} \approx 5$ km s^{-1}). Ayres and Linsky proposed that the connection between the fast rotation of the secondary and its enhanced ultraviolet emissions paral-

[1] Guest Observer, *International Ultraviolet Explorer*.

lels the empirical rotation-activity relation in Ca II flux described by Wilson (1966), Kraft (1967), Skumanich (1972), and others: the chromospheric emissions very likely form in regions on the stellar surface disturbed by magnetic activity, itself strongly tied to rotation and envelope convection through the "dynamo" mechanism (e.g., Parker 1970). Thus, Capella serves as a paradigm of the rotation-activity connection.

Furthermore, the factor of ~ 7 smaller rotation rate of Capella Aa compared with Ab emphasizes the remarkable influence that evolution can have on the fundamental properties of moderate-mass stars ($M \approx 3\ M_{\odot}$) as they pass rapidly through the Hertzsprung gap, ascend into the red giant branch, and finally loop back to a prolonged residence in the core-helium-burning (CHeB) "clump" near K0 III. Thus, Capella also serves as a paradigm of dramatic evolutionary changes in the Hertzsprung gap.

The present work focuses on the detailed spectral differences between the giants of Capella in the vacuum ultraviolet, characterized by emissions from the stellar outer atmosphere over a broad range in temperature from about 6×10^3 K to a few $\times 10^5$ K. Further, the "spectral dissection" described in the present study represents a powerful technique that can be applied to other analogous, but fainter, binary systems (e.g., Eriksson *et al.* 1986).

II. OBSERVATIONS

a) Overview

The observational goal of the present study was to isolate the individual contributions of Capella Aa and Ab in composite ultraviolet spectra of the system. The full orbital velocity swings of the stars between the radial velocity extrema (quadratures) are comparable to, or larger than, the Doppler widths of most of the important emission lines. Thus, one can align spectra from opposite quadratures to the reference frame of either of the stars, and difference the spectra to eliminate the contribution of that star.

b) The Observations

I conducted the observing program in two, essentially identical, parts: the first on 1985 November 15 at orbital phase $\phi = 0.261$–0.266; and the second on 1986 January 4 at orbital phase $\phi = 0.740$–0.746 (the ephemeris is cited in Table 1: $\phi = 0$ is the conjunction with the primary [the more massive star] in front). Each part consisted of a series of 0.1–0.3 Å resolution echelle spectra in the 1150–2000 Å region (SWP camera) and in the 2000–3200 Å region (LWP camera): specifically, matched pairs of large-aperture (10″ × 20″ oval) exposures, with the stellar image alternately placed $\sim 5''$ to either side of the center of the aperture, along the echelle dispersion axis; followed by one or more exposures through the small aperture (3″ diameter).

The exposures at off-center positions in the large aperture, and through the small aperture, enable one to apply techniques to compensate for some of the more troublesome defects of *IUE* images: cosmic particle radiation spikes, hot pixels, and reseau marks. Such defects will appear at different locations in each spectrum with respect to the stellar emission lines and can be filtered by numerical comparison procedures.

The exposure times were 90 minutes for the SWP large-aperture spectra, and 90 seconds for the LWP spectra. The small-aperture exposure times typically were twice those of the large-aperture spectra. I also took a few short SWP echellograms to record important features, like Si III] λ1892, that were heavily overexposed in the deeper SWP observations.

A catalog of the *IUE* exposures is provided in Table 1.

TABLE 1

CATALOG OF *IUE* EXPOSURES

Image No.	Offset Ref. Pt. (FES units)	t_{exp} (minutes)	JD 2,446,000+
Orbital Phase[a] $\phi = 0.261$–0.266			
L7108	(−37, −207)	1.5	385.35
S27119	(−37, −207)	90	385.39
L7109	(+05, −209)	1.5	385.42
S27120	(+05, −209)	90	385.51
L7110	sa	3 × 50s[b]	385.56
S27121	sa	3 × 60[b]	385.66
L7111	sa	3.0	385.62
L7112	sa	3.0	385.68
L7113	sa	3.5	385.77
S27122	sa	3 × 10[b]	385.81
S27123	sa	18sλcal	385.84
L7114	sa	16sλcal	385.85
S27124	(−37, −207)	15	385.88
Orbital Phase[a] $\phi = 0.740$–0.746			
L7455	(−37, −207)	1.5	435.20
S27445	(−37, −207)	90	435.24
L7456	(+05, −209)	1.5	435.30
S27446	(+05, −209)	90	435.34
L7457	sa	3 × 1.5[b]	435.40
S27447	sa	3 × 15[b]	435.46
L7458	sa	16sλcal	435.48
S27448	sa	3 × 30[b]	435.56
S27449	sa	18sλcal	435.64
S27452	(−37, −207)	15	435.75

NOTE.—All exposures in high-dispersion mode through the large aperture (10″ × 20″), unless otherwise noted: "sa" indicates an exposure through the small aperture (3″ diameter); "λcal" indicates an exposure of the Pt-Ne hollow cathode lamp through the small aperture with the large-aperture shutter closed, on top of a 5 s TFLOOD (flat-field lamp exposure). The center of the large aperture is at Offset Reference Point (−16, −208). In the second series of observations, two low-dispersion exposures (SWP 27450 and SWP 27451) also were taken, but not reduced for this study.

[a] The ephemeris for Capella is based on that cited in Batten, Fletcher, and Mann (1978): JD = 2,442,093.347 + 104.0204 × *E*, where zero phase is the conjunction with the spectroscopic primary (Aa) in front.

[b] Several of the small-aperture observations were conducted in three equal-length parts, with the stellar image repositioned at the beginning of each. The procedure was intended to randomize the small centering error associated with the short slew from the reference point of the fine error sensor (FES).

III. DATA REDUCTION AND ANALYSIS

a) Flux and Wavelength Calibrations

I calibrated the stellar spectra using standard procedures at the *IUE* Regional Data Analysis Facility in Boulder (e.g., Schiffer 1982); the echelle blaze correction constants derived by Ake (1982); the low-dispersion inverse sensitivity of Bohlin and Holm (1980) as updated by Holm *et al.* (1982); and the high-dispersion to low-dispersion exposure ratios for *continuum* sources appropriate to the prevailing configuration of the Spectral Image Processing System (Cassatella, Ponz, and Selvelli 1983).

I established a common wavelength scale for each independent series of SWP exposures according to a set of 12 prominent emission features well-distributed across the echelle

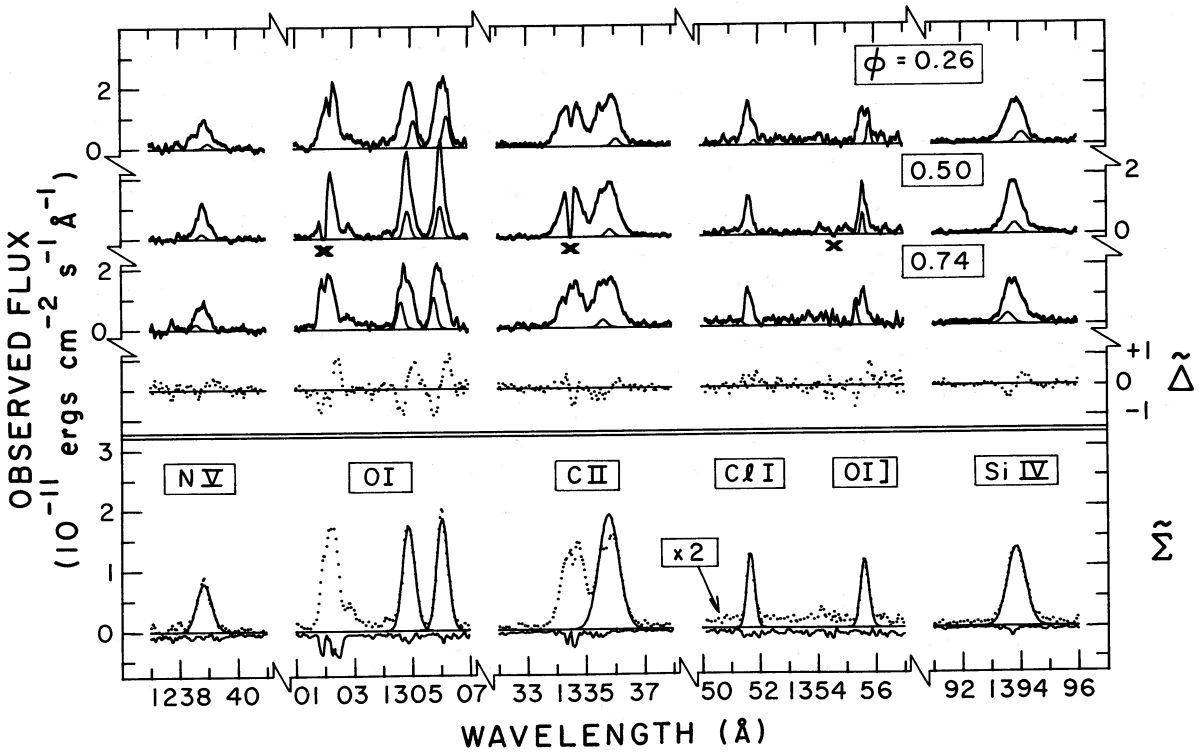

FIG. 1*a*

FIG. 1*a*.—Comparison of SWP spectra of Capella taken at critical orbital phases. The three sets of heavily drawn tracings in the upper panel illustrate the co-added spectra in the vicinity of important stellar emission features on a wavelength scale registered to the frame of reference of the active secondary star (Capella Ab). Note that the 1982 spectra ($\phi = 0.50$) contain regions that are corrupted by camera reseaux (marked by crosses below tracing): these are entirely eliminated in the new spectra owing to the redundant sampling of different parts of the vidicon detectors for each effective wavelength. The dotted curves in the lower portion of the upper panel depict the *difference* ($\tilde{\Delta}$) between the spectra taken at $\phi = 0.26$ and $\phi = 0.74$ (radial velocity extrema). The "difference signatures" due to the primary spectrum are seen clearly in most of the features: the inferred line shapes, based on modeling the signatures, are depicted as smooth curves at the appropriate velocity shifts under the observed spectra. The bottom panel illustrates, as dotted curves, the result of correcting the three sets of spectra for the small contribution due to the primary and adding them in the reference frame of the secondary star. The solid curves *below* the phase-averaged SWP spectra illustrate the point-by-point rms of the summation (plotted as −rms). The rms not only is an empirical measure of the local noise level, but it also can contain significant structure due to features that are *not* in the reference frame of the secondary, and were not properly treated in the correction procedure. Notice, for example, the structure in the shortward components of the O I and C II multiplets produced by the (uncorrected) emissions of the primary star and absorptions of the interstellar medium. The smooth, solid curves in the lower panel are Gaussians fitted to the corrected phase-averaged profiles of Capella Ab. Note the pronounced "red asymmetry" of the core of C II λ1335.

format. I measured the apparent wavelengths by means of a least-squares Gaussian fitting technique (e.g., Ayres *et al.* 1983). In pair-wise comparisons, I calculated the differential velocity shift over the ensemble of reference lines, weighting them according to the square of their statistical significance ($\varpi_L = [f_L/\sigma_f]^2$).

I treated the LWP spectra in a similar manner, except that I registered the small-aperture and off-center large-aperture spectra by numerically cross-correlating eight absorption-line regions (each ~10 Å wide) from five echelle orders ($m = 80$–84) centered on the important Mg II λ2800 doublet.

In addition to the new spectra, I reanalyzed five pairs of short (22.5 minutes) and long (80–137 minutes) exposures I took in 1982 December at single-line phase $\phi = 0.50$ (see Ayres 1984). The SWP images in the 1982 series were taken with Capella centered in the large aperture, and unfortunately no longwavelength observations were included.

b) Combining the Spectra

Having translated the individual spectra, at a particular orbital phase, to a common wavelength scale, I co-added them using the "difference filter" technique described in Ayres *et al.* (1986) and Ayres, Jensen, and Engvold (1988). The algorithm effectively removes cosmic-ray spikes; extends the dynamic range (when exposures of different duration are combined); and improves the signal-to-noise ratios.

The filtered, co-added SWP spectra at the three critical orbital phases are illustrated in Figures 1*a* and 1*b*. The two sets of LWP spectra, in the region of the important Mg II λ2800 doublet, are shown in Figure 2.

c) Velocity of the Local Interstellar Medium in the Direction of Capella

One experiment that can be performed readily with the three sets of co-added SWP spectra is the determination of the velocity of the local interstellar medium in the direction of Capella.

I aligned the SWP spectra to one another, in the reference frame of Capella Ab, according to numerical cross-correlation of prominent absorption structure in several echelle orders in the 1800–2000 Å region, where the hotter secondary completely dominates the continuum emission. I assigned a common wavelength scale based on that from the $\phi = 0.50$ single-line phase, which I registered to the weighted-mean velocity of a set of narrow, low-excitation emission features from multiplets of neutral carbon, oxygen, sulfur, and chlorine (cf. Ayres, Jensen, and Engvold 1988).

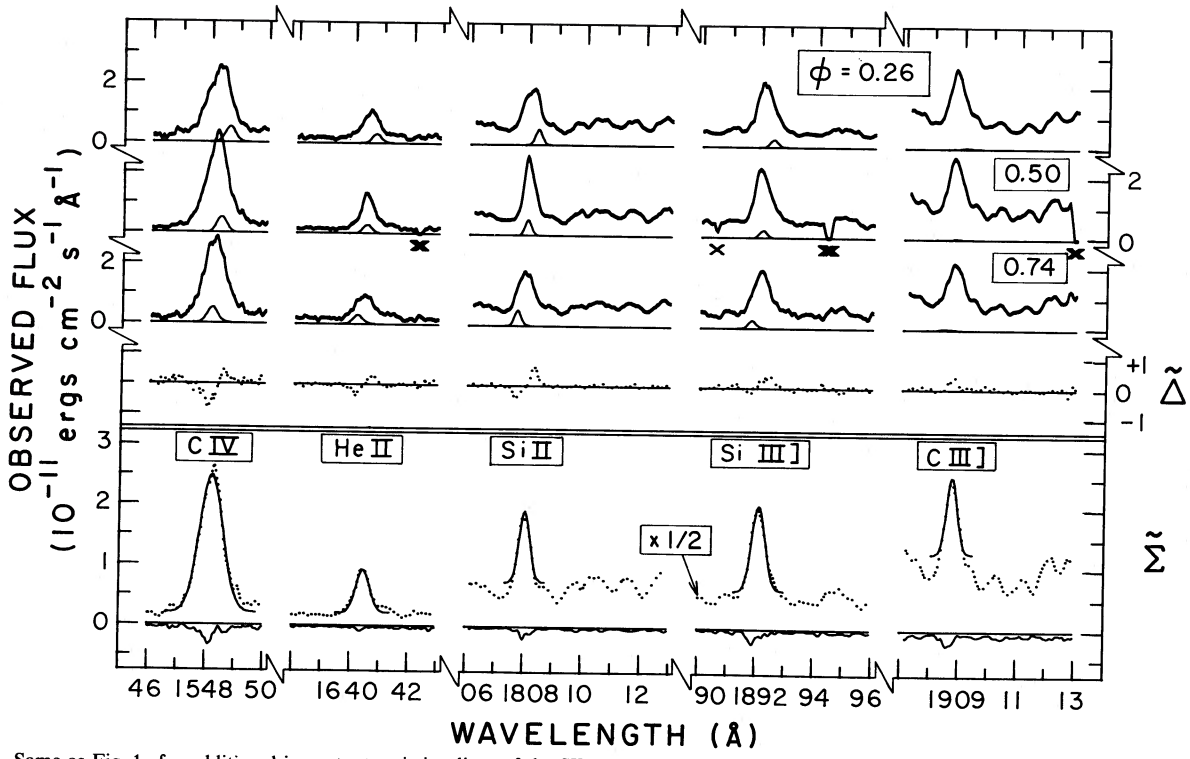

FIG. 1*b*.—Same as Fig. 1*a* for additional important emission lines of the SWP region. Note the lack of discernable difference signatures corresponding to the pronounced absorption structure outside of the emission lines in the region longward of 1800 Å: the hotter secondary star completely dominates the continuum emission in this part of the spectrum.

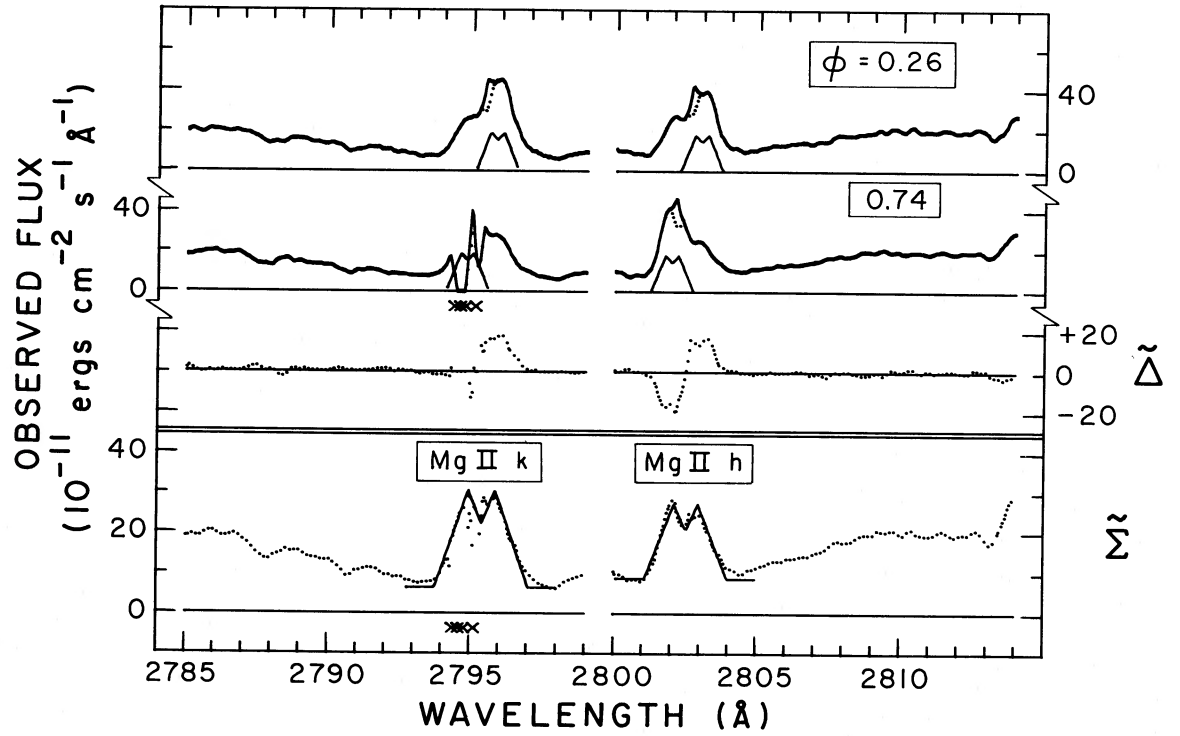

FIG. 2.—Analogous to Fig. 1 for the chromospheric Mg II *h* and *k* lines of the LWP region. No long-wavelength observations were taken in the 1982 ($\phi = 0.50$) series, consequently no rms was constructed. Note that the central portion of the Mg II *k* emission core in the $\phi = 0.74$ series is affected by saturation. The presence of *absorption* difference signatures (e.g., near 2788 Å) indicates the increasing visibility of the cooler primary spectrum towards longer wavelengths. In the extreme cores of the *h* and *k* profiles of the upper panel, the short dotted curves illustrate the original co-added spectra in the vicinity of the interstellar Mg II absorptions, and the solid curves depict the corrected spectra. Note also that the fitting functions for the stellar Mg II features are trapezoidal, with shallow central reversals, rather than Gaussian.

Next, I shifted each of the quadrature spectra ($\phi = 0.26$, 0.74) relative to the single-line phase ($\phi = 0.50$) according to the predicted orbital velocity of the secondary star ($K_2 = 27.5$ km s^{-1}: Batten, Fletcher, and Mann 1978). By doing so, the three spectra were aligned in the center-of-mass reference frame (more precisely, the "γ" velocity determined by chromospheric emission lines). I then combined the three co-added spectra: any features that are "stationary" in the γ-frame—like the interstellar medium—are emphasized in the sum, while "moving" features—like those of Capella Aa and Ab—are blurred.

I modeled the blurred emission profiles of the lines that exhibited prominent, sharp interstellar absorption features: D I λ1215 (in H I Lyα), O I λ1302, and C II λ1334. Gaussian profiles proved to be adequate in all cases. I subtracted the fitted emission profiles from the phase-averaged line shapes to compensate for the sloping backgrounds against which the interstellar absorptions are viewed. Finally, I measured the residual absorption features. The results are listed in Table 2. If the chromospheric γ-velocity is identical to the well-determined optical γ-velocity (+29.5 km s^{-1}: Batten, Fletcher, and Mann 1978), then $v_{ISM} = +20 \pm 1$ km s^{-1} in the direction of Capella.

The preceding result was of practical value: the accurate alignment of the LWP wavelength scales in the Ab frame by spectral cross-correlation *between the quadratures* was prevented by increased contamination by the cooler primary spectrum. I therefore established the common wavelength scale for the two series of co-added LWP spectra according to the apparent velocities of the interstellar components of Mg II *h* and *k*.

d) Isolation of the Primary Spectrum

In order to isolate the spectrum of the primary star, I aligned the $\phi = 0.26$ and $\phi = 0.74$ SWP and LWP spectra in the frame of reference of the secondary, and subtracted them to cancel its broad, bright emission features. The resulting differences are illustrated in Figures 1 and 2. The influence of the faint primary spectrum in the region shortward of 2000 Å is obvious in many of the features, particularly the chromospheric emissions like the O I triplet near 1305 Å and Si II λ1808, and to a lesser extent the higher excitation emissions like He II λ1640, Si IV λ1393, and C IV λ1548. The influence of the primary is more obvious in the Mg II doublet, although the difference signature in the *k* line is affected by the saturated core for $\phi = 0.74$. Curiously, the residuals for the important density-sensitive lines Si III] λ1892 and C III] λ1908 appear to be distorted, as if the primary spectrum exhibited some variability between the two series of observations.

TABLE 2

INTERSTELLAR LINES IN SWP REGION

Transition	λ_0	m	$v_L - v_{low\text{-}ex}$	FWHM
D I	1215.339	114	-5.7 ± 0.7	38
D I	1215.339	113	-9.6 ± 1.2	42
O I	1302.169	106	-9.5 ± 0.9	18
C II	1334.532	103	-12.6 ± 1.4	33
$\langle v_{ISM} \rangle - v_{low\text{-}ex}$:			-9.4 ± 1.2	

NOTE.—Line parameters were determined by a least-squares Gaussian modeling procedure (see text). Rest wavelengths (λ_0: Å in vacuum) are from Kelly (1982); m is the echelle order number; velocities, in km s^{-1}, are in the chromospheric "γ"-velocity frame (see text); line widths also in km s^{-1}. Errors (1 σ) in line positions are based on variance of the fitted profile from the true data points. The uncertainty in the average velocity is 1 standard error of the mean.

i) *Fitting the Difference Signatures: SWP Region*

I developed a least-squares fitting procedure, based on Gaussian line shapes, to model the residuals in the SWP difference spectra, in the spirit of the technique used by Ayres and Testerman (1981) to model *ratio* signatures of solar molecular *absorption* lines (recorded at opposite equatorial limbs of the Sun and shifted relative to terrestrial features by solar rotation). The fixed parameter in the modeling scheme is the full velocity shift of the primary star relative to the secondary between the quadratures, i.e., $2 \times (K_1 + K_2) = 107$ km s^{-1} (Batten, Fletcher, and Mann 1978). The variable parameters are the full width at half-maximum intensity (FWHM), the integrated line flux (f_L), and the apparent wavelength of the feature (λ_L) in the rest frame of the primary star: these were assumed to be independent of phase.

For the several cases of well-defined difference signatures, the procedure is deterministic and the uncertainties in the derived line-shape parameters are small. However, when the difference signature is quite noisy or exhibits only a single lobe, the procedure is less certain, and might provide merely an upper limit to the integrated flux of the primary. Further, O I λ1302 and C II λ1334 are affected by distinct interstellar absorption features, which appear to shift between the quadratures because the spectra are aligned in the reference frame of the secondary. Since at least one other member of each multiplet, free of the interstellar features, was available for modeling, I did not attempt to correct the principal components for the ISM absorptions.

ii) *Fitting the Difference Signatures: LWP Region*

For Mg II *h* and *k*, I developed a somewhat more elaborate scheme. There, *both* components of the multiplet are affected by interstellar absorptions. Furthermore, the residuals indicate that the underlying shapes of the stellar Mg II profiles are distinctly *non*-Gaussian: indeed, they appear to have pronounced central reversals. I therefore corrected the initial profiles for a Gaussian absorption due to interstellar Mg^+, and treated the primary components as trapezoids with triangular central dips (cf., Ayres, Schiffer, and Linsky 1983). Although the modified scheme involves additional free parameters, the high signal-to-noise ratios of the LWP spectra and the larger contribution by Capella Aa at Mg II, render it quite tractable.

iii) *Pristine Spectra of Capella Ab*

Having obtained quantitative estimates of the influence of Capella Aa, I corrected the observed blended profiles at each orbital phase for that contribution: what remained should be the true line shapes of the secondary. I then combined the recovered secondary profiles from the available orbital phases (3 for the SWP; 2 for the LWP) to produce the phase-averaged spectra illustrated in the lower panels of Figures 1 and 2. The summation ignored any regions of the individual spectra which were affected by saturated pixels or reseau marks not removed in the difference-filtering procedure. I then fitted the resulting phase-averaged profiles of the secondary with least-squares Gaussian line shapes. I applied a similar approach to the LWP spectra of the Mg II *h* and *k* lines, with the modified fitting function described previously.

Tables 3*a* and 3*b* summarize the far-ultraviolet properties of the primary and secondary spectra of Capella; Table 4 summarizes the Mg II properties.

TABLE 3A

FAR-UV LINE PARAMETERS FOR CAPELLA Aa

Transition	λ_L	FWHM	FWHM(β)	f_L	f_{Aa}/f_{Ab}
Low-Excitation Lines					
O I	1304.9	60	(60)	2.5 ± 0.7	0.27
O I	1306.0[a]	60	(60)	2.9 ± 0.5	0.32
O I	1306.0[b]	60	(60)	2.5 ± 0.4	0.24
Cl I	1351.6	40	(...)	$\lesssim 0.6$	$\lesssim 0.3$
O I]	1355.6	30	(40)	0.5 ± 0.2	0.24
Si II	1808.0	45	(45)	1.5 ± 0.3	0.28
Moderate-Excitation Permitted Lines					
Si III	1206.5	110	(170)	4.3 ± 0.8	0.13
C II	1335.8	70	(70)	0.8 ± 0.4	0.05
He II	1640.4	70	(70)	1.2 ± 0.3	0.28
High-Excitation Intersystem Lines					
Si III]	1892.1	50	(50)	$\lesssim 2.2$	$\lesssim 0.1$
C III]	1908.8	60	(60)	$\lesssim 1.6$	$\lesssim 0.3$
High-Excitation Permitted Lines					
N V	1238.8	70	(60)	$\lesssim 1.2$	$\lesssim 0.2$
Si IV	1393.8	90	(60)	1.6 ± 0.3	0.15
C IV	1548.4	80	(70)	2.3 ± 0.7	0.10

NOTE.—Line parameters were determined by a least-squares Gaussian modeling procedure applied to the residual "difference signatures" obtained by subtracting spectra of Capella, from opposite orbital quadratures, in the reference frame of the active secondary. Errors (1 σ) in the line fluxes are based on the variance of the fitted signature from the true data points. λ_L is the derived line-center wavelength (Å) in the reference frame of the primary; FWHM (km s^{-1}) is the derived line width. FWHM(β) are typical line widths taken from high-dispersion *IUE* spectra of β Ceti and β Geminorum, two K0 stars thought to be similar to the Capella primary. Line fluxes—f_L—are in units of 10^{-12} ergs cm^{-2} s^{-1}; upper limits (indicated by "$\lesssim$") are 2 σ.

[a] Echelle order 106.

[b] Echelle order 105.

e) *Physical Properties of Capella Aa and Ab*

In their early *IUE* study of Capella, Ayres and Linsky (1980) deduced the fundamental stellar parameters of the primary and secondary according to: (1) broad-band photometric indices, ranging from the far-ultraviolet (*OAO 2* radiometry) to the optical and near infrared (Johnson [1966] *UBVR* colors); and (2) the difference in visual magnitudes, $\Delta V \equiv V_{Aa} - V_{Ab} \approx -0.25$ mag (i.e., primary brighter than secondary by about 25% in the visual region), estimated by Wright (1954). The derived spectral types were mid-G ($\sim$G6) for the primary, and late-F ($\sim$F9) for the secondary; consistent with Wright's (1954) original assignment of G5 III and G0 III.

Recently, Griffin and Griffin (1986) published a short note concerning the spectral properties of Capella based on a Coravel-type photoelectric radial velocity measurement near an orbital quadrature of the binary. The Griffins concluded that the difference in visual magnitudes should be $\Delta V \approx +0.15$ mag *in favor of the secondary.*

In the context of the Ayres-Linsky work, the brighter relative visual magnitude of the secondary proposed by the Griffins slightly reddens its spectral type, to about G1. The primary remains near G5. Table 5 summarizes the fundamental stellar parameters based on the revised ΔV.

IV. DISCUSSION

a) *The Rotation-Activity-Evolution Connection*

An *IUE* study of the far-ultraviolet emissions of field yellow giants by Simon (1984) showed that $f_{C\,IV}/f_{bol}$—a measure of subcoronal activity—rises rapidly through the F giants; peaks near G0; and falls precipitously toward the later spectral types: there, a dispersion of approximately an order of magnitude in the normalized C IV emission is found in the range G5–K0 at luminosity class III. Gray (1982) previously reported a similar behavior in the mean rotation rates of the yellow giants: $\langle v \sin i \rangle$ is large among the F and early-G giants, but falls rapidly toward mid- and late-G.

The rise in activity in the F giants very likely signals the initial development of a thick convection zone, in which dynamo action can proceed efficiently in rapidly rotating stars (e.g., Simon 1984). The sharp decline in rotation (and therefore also activity) toward the later spectral types generally is attributed to internal *redistribution* of angular momentum (Gray and Endal 1982), if only because the first crossing is too brief ($\sim 0.01\tau_{MS}$) to permit significant *loss* of angular momentum.

Since the rotation rate of the Capella primary is slow, while that of the less evolved secondary is fast, a careful assessment of the true position of the primary on its evolutionary trajectory is useful for testing detailed models of angular momentum redistribution, or other spindown mechanisms like the braking action of a coronal wind (e.g., Durney 1972).

TABLE 3B

FAR-UV LINE PARAMETERS FOR CAPELLA Ab

Transition	$v_L - v_{low\text{-}ex}$	FWHM	f_L	f_C
Low-Excitation Lines				
S I 1295[a]	-2.9 ± 1.0	87	2.1 ± 0.1	0
O I 1304	7.5 ± 1.0	114	9.1 ± 0.4	0
O I 1306[b]	4.4 ± 1.2	107	9.2 ± 0.4	0
O I 1306[c]	5.6 ± 0.7	103	10.5 ± 0.3	0
Cl I 1351[a]	1.5 ± 1.1	71	2.1 ± 0.1	0
O I] 1355[a]	3.6 ± 1.1	78	2.1 ± 0.1	0
Si II 1808	4.9 ± 1.0	71	5.4 ± 0.3	7.4
Moderate-Excitation Permitted Lines				
Si III 1206[a]	-0.2 ± 1.2	233	33.7 ± 0.8	0
C II 1335[a]	13.2 ± 0.7	182	16.4 ± 0.3	0
He II 1640	11.3 ± 0.8	103	4.4 ± 0.2	2.1
$\langle v_L \rangle - v_{low\text{-}ex}$: .	$+8.7 \pm 4.8$			
High-Excitation Intersystem Lines				
Si III] 1892[a]	12.4 ± 0.9	86	16.3 ± 0.7	12.7
C III] 1908[a]	6.2 ± 0.9	69	6.0 ± 0.3	12.7
$\langle v_L \rangle - v_{low\text{-}ex}$: .	$+10.1 \pm 2.7$			
High-Excitation Permitted Lines				
N V 1238	4.4 ± 2.6	146	5.1 ± 0.4	0
Si IV 1393[a]	16.5 ± 0.8	161	10.4 ± 0.2	0
Si IV 1402[a]	6.9 ± 2.0	156	5.9 ± 0.3	0
C IV 1548[a]	0.9 ± 1.4	184	23.1 ± 0.8	2.0
C IV 1550[a]	18.2 ± 1.1	148	13.0 ± 0.4	2.0
$\langle v_L \rangle - v_{low\text{-}ex}$: .	$+13.1 \pm 3.7$			

NOTE.—Line parameters were determined by a least-squares Gaussian modeling procedure. Errors (1 σ) are based on variance of the fitted profile from the true data points. Velocities and FWHMs are in km s^{-1}. The formal uncertainties in the FWHMs are approximately twice those of v_L. Line fluxes—f_L—are in units of 10^{-12} ergs cm^{-2} s^{-1}; continuum fluxes—f_C—are in units of 10^{-12} ergs cm^{-2} s^{-1} Å^{-1}.

[a] Lines included in (velocity) average over that excitation group: weighting was according to $(f_L/\sigma_f)^2$. The uncertainty in $\langle v_L \rangle - v_{low\text{-}ex}$ is the quadratic sum of the two standard errors.

[b] Echelle order 106.

[c] Echelle order 105.

TABLE 4

MID-UV Mg II *h* AND *k* LINES OF CAPELLA

PARAMETER	Aa	Ab
	Mg II λ2795.5 [*k*]	
ΔV_{top}	50 ± 3	100 ± 5
ΔV_{base}	160 ± 10	350 ± 15
Central dip	0.20	0.35
$(f_\lambda)_{base}$	0	64
f_{k1}	180 ± 10	680 ± 25
	Mg II λ2802.7 [*h*]	
ΔV_{top}	50 ± 3	90 ± 5
ΔV_{base}	160 ± 10	310 ± 15
Central dip	0.20	0.35
$(f_\lambda)_{base}$	0	86
f_{h1}	170 ± 10	570 ± 20

NOTE.—The first two parameters are widths, in km s^{-1}, characterizing the trapezodial profiles adopted in the modeling procedure; the third parameter is the relative depth of the triangular central reversal (see, e.g., Fig. 2); the fourth parameter is a constant background level upon which the Mg II emissions of the star are assumed to sit: the units are 10^{-12} ergs cm^{-2} s^{-1} $Å^{-1}$; the final parameter is the total flux integrated between the k_1 (or h_1) minimum features in units of 10^{-12} ergs cm^{-2} s^{-1}, including the contribution from the "base flux."

i) *The Evolutionary Status of the Primary*

Wallerstein (1966) and Boesgaard (1971) reported a near absence of Li I λ6708 absorption in the primary, suggesting that it already has experienced deep convective mixing—the major mechanism for diluting surface lithium—which occurs during the first ascent of the red-giant branch (Iben 1965).

In parallel to the depletion of lithium, surface enrichments of isotopic carbon (^{13}C) and isotopic oxygen (^{17}O, ^{18}O) accompany the mixing episodes immediately prior to, and following, core helium ignition (e.g., Lambert 1981). Near-infrared spectra of cyanogen (CN) absorptions in the sharp-line (primary) spectrum indicate $^{12}C/^{13}C = 27$, similar to the average isotopic ratio—21—of the four clump giants of the Hyades (Tomkin, Luck, and Lambert 1976).

TABLE 5

FUNDAMENTAL STELLAR PARAMETERS

PARAMETER	Aa	Ab
$(V-R)$ (mag)	0.66 ± 0.02	0.55 ± 0.02
Sp. Type $(V-R)$	G5 (G4-G8)	G1 ± 1
T_{eff} (K)	5100 ± 100	5700 ± 100
m_v (mag)	0.91	0.76
f_{bol} (10^{-7} cgs)	135	135
$L/L_\odot$	74	74
$R/R_\odot$	11	9
$M/M_\odot$	3.3 − 3.2	2.8 − 3.0
$v \sin i$ (km s^{-1})	5 ± 2	36 ± 3
age (yr)	$2.5–3 \times 10^8$	

NOTE.—Stellar parameters through $R/R_\odot$ obtained assuming $V_{Aa} - V_{Ab} \approx +0.15$ mag (Griffin and Griffin 1986), and a distance of 13.2 pc (Heintz 1975). Masses from Shen *et al.* (1985: $M_{Aa}/M_{Ab} = 1.18 \pm 0.02$ [first entries]); or Fekel, Moffett, and Henry (1986: $M_{Aa}/M_{Ab} = 1.07 \pm 0.02$ [second entries]). Rotational velocities from Fekel, Moffett, and Henry (1986) and Griffin and Griffin (1986). The ages (for a 3 $M_\odot$ star in its first crossing of the Hertzsprung gap) are from Iben (1965) and Lattanzio (1986).

Both the severe dilution of lithium and the enrichment of isotopic carbon imply that Capella Aa is in the core-helium-burning phase. In principle, accurate measurements of the slight mass difference between the primary and secondary should constrain the true "distance" between their current positions on the evolutionary trajectories, and reveal whether the primary is a recent arrival to the clump, or a well-established resident.

An analysis by Fekel, Moffett, and Henry (1986), peripheral to an extensive survey of close-binary systems, obtained $M_{Aa}/M_{Ab} = 1.07 \pm 0.02$. Their result substantiates the 5% mass difference derived by Wright (1954), and places the primary more than midway through the clump phase, according to the chronology of Iben (1965) for 3 $M_\odot$ stars. In another recent radial-velocity study, using a Coravel-type technique, Shen *et al.* (1985) reported $M_{Aa}/M_{Ab} = 1.18 \pm 0.02$. Their mass ratio not only is significantly larger than those of all previous work, but it also conflicts seriously with Iben's (1965) evolutionary models: for a main-sequence (core-hydrogen-burning) lifetime of,

$$\tau_{MS} \approx 2.5 \times 10^8 (M/3\ M_\odot)^{-2.7}\ \text{yr}\ , \quad (1)$$

the 7×10^7 yr duration of the core-helium-burning phase at 3 $M_\odot$ would prevent two coeval stars differing by more than 10% in mass from simultaneously occupying the yellow-giant region of the H-R diagram.

Recently, Lattanzio (1986) published an extensive series of evolutionary tracks for stars in the mass range 1–3 $M_\odot$. For a similar helium abundance to that used by Iben ($Y = 0.3$), Lattanzio obtains a slightly longer MS lifetime,

$$\tau_{MS} \approx 3 \times 10^8 (M/3\ M_\odot)^{-2.7}\ \text{yr}\ , \quad (2)$$

but a significantly longer core-helium-burning time, $\sim 2 \times 10^8$ yr; nearly 3 times that of Iben, and comparable to τ_{MS} itself. If the clump residence time truly is as long as indicated by Lattanzio's calculations, then the large mass ratio for Capella obtained by Shen *et al.* is plausible: indeed, the primary would have completed only about 50% of its clump lifetime.

Aside from the differences between the Iben and Lattanzio evolutionary tracks, the disagreement between the two independent radial-velocity studies is uncomfortably large. Until these differences are resolved, the important question concerning whether the primary is a recent arrival to the clump, or a long-term resident, will not be settled.

ii) *Comparison of Capella Aa to Other Clump Giants*

It is enlightening to compare the ultraviolet properties of Capella Aa to stars of similar evolutionary status. Perhaps the best comparison is with the four ~K0 giants of the Hyades open cluster, which have been studied extensively from the ground (e.g., Gray and Endal 1982) and with the *IUE* (Baliunas, Hartmann, and Dupree 1983: BHD). Indeed, Capella shares the space motion of the cluster (Eggen 1960), and quite possibly is coeval. I also have included in the comparison the K0 giants β Geminorum and β Ceti, stars of enhanced C IV and X-ray emissions compared to the cooler red giants like α Bootis (K1 III) and α Tauri (K5 III) (Ayres *et al.* 1981), but very likely also clump stars like the Hyades giants (cf. Simon 1984). In terms of $f_{C\,IV}/f_{bol}$, the six reference stars fall into two distinct classes: an active group—β Ceti, γ Tauri, and θ^1 Tauri; and a less active group—β Gem, δ^1 Tauri, and ε Tauri.

TABLE 6

COMPARISONS WITH OTHER CLUMP GIANTS

Parameter	Capella Ab	Capella Aa	β Cet type	β Gem type
$L/L_\odot$	74	74	57 ± 14	61 ± 17
$(V-R)$ (mag)	0.55	0.66	0.72 ± 0.01	0.74 ± 0.01
Spectral type	G1	G5	K0	K0
$v \sin i$ (km s^{-1})	36	5	3[a]	3[a]
Transition	f_L/f_{bol} (10^{-7})			
O I 1305	20	5.2	4.2 ± 1.4	1.2 ± 0.2
C II 1335	18	0.9	0.9 ± 0.4	0.09 ± 0.02
Si IV 1400	12	1.8	1.1 ± 0.6	0.19 ± 0.07
C IV 1550	30	2.9	1.4 ± 0.5	0.23 ± 0.04
He II 1640	3.7	1.0	0.7 ± 0.2	<0.05
Si II 1816	18	5.0	3.5 ± 0.6	1.1 ± 0.2
f_C[1900 Å]	$\lesssim 7.2$	...	0.63 ± 0.23	0.16 ± 0.07

NOTE.—The uncertainties cited for the β Cet type (β Cet; γ Tau; θ^1 Tau) and β Gem type (β Gem; δ^1 Tau; ϵ Tau) are *standard deviations* (1 σ) to illustrate the *variance* of the values within each group. The 1900 Å continuum flux—f_C—was measured in each SWP-LO spectrum after all emission line structure was removed by a filtering procedure. The luminosities of the Hyads were calculated for $d = 44$ pc; for the other stars, parallactic distances were used.

[a] Hyads, only (from Baliunas, Hartmann, and Dupree 1983).

I determined mean normalized fluxes of representative emission features by collecting all of the line detections, or 2 σ upper limits, of the six stars from the extensive *IUE* SWP-LO survey by Bennett (1987). For each star, I averaged f_L/f_{bol} over the available measurements, ignoring lines that were grossly underexposed or overexposed. If only upper limits were available for a particular line, the smallest was selected. The normalized fluxes of the reference lines then were averaged over the three stars of each activity group: upper limits for the comparatively faint Hyads often could be replaced by a detection, or a smaller upper limit, from the bright prototype stars.

The "β Cet type" stars have chromospheric emissions (e.g., O I and Si II) 3–4 times stronger than those of the "β Gem type"; and higher excitation emissions (e.g., C II, Si IV, and C IV) 5–10 times stronger. The continuum flux at 1900 Å also is enhanced in the β Cet group compared with the β Gem stars: the larger f_{1900}/f_{bol} likely reflects the slightly bluer average $(V-R)$ color of the β Cet group, despite the fact that all six stars are classified essentially as K0.

BHD suggested that the enhanced ultraviolet emissions of γ Tau and θ^1 Tau might be related to unseen dwarf companions; if F-type stars, these could contribute significantly to the high-excitation lines as well as to the photospheric continuum in the 1900 Å region (cf. Ayres 1985). However—following an argument originally advanced by BHD—the ratio of chromospheric O I/Si II emission in γ Tau and θ^1 Tau (as well as in δ^1 Tau and ϵ Tau) is greater than 1; whereas in active dwarf stars, O I/Si II is less than ~ 0.3, probably because Lyβ pumping of the oxygen triplet is less effective in high-density chromospheres (cf. Ayres, Marstad, and Linsky 1981). Thus, the β Cet type (and the β Gem type) Hyads exhibit chromospheric emission ratios that are compatible with their luminosity classes. The relative emission levels of the higher excitation species, in turn, very likely are intrinsic to the giants, themselves, rather than to "hyperactive" dwarf companions.

BHD also suggested that the differences in the emission levels of the Hyades giants might be due to the operation of stellar activity cycles: one simply has sampled high points in some of the cycles, and low points in the others. While this possibility cannot be ruled out, I find it unlikely in view of the rather small variability ($\lesssim 50\%$) exhibited by chromospheric and higher excitation lines over the *solar* cycle (see, e.g., Bennett 1987): the normalized fluxes of the β Cet type Hyads are quite comparable to those of the Sun.

Although the β Cet type and β Gem type groups were established here mostly for convenience, the prototypes of the two classes also exhibit distinctly different behavior in chromospheric He I λ10830 absorption (O'Brien and Lambert 1986; Lambert 1987): β Ceti shows strong, possibly variable, and possibly redshifted λ10830 absorption with $W_\lambda \approx 300$–500 mÅ; while β Gem shows little or no variability in a shallow absorption profile with $W_\lambda \approx 120$ mÅ. Modeling by O'Brien and Lambert suggests that the two giants have significantly different surface coverages by magnetic active regions; an explanation that could be applied equally well to the dichotomy in far-ultraviolet emissions.

Capella Aa clearly belongs to the β Cet group in terms of its chromospheric and higher excitation emissions, as well as its large λ10830 absorption equivalent width, $W_\lambda = 500 \pm 60$ mÅ (O'Brien and Lambert 1986).

Perhaps the β Cet type Hyads and the Capella primary are in the early stages of core-helium burning; while the β Gem type Hyads are a few tenths of a $M_\odot$ more massive and in a more advanced phase, on the redward branch of the "blue loop" that develops for solar-composition stars near 3 $M_\odot$ (see, e.g., Lattanzio [1986], his Fig. 1).

If the β Gem type Hyads are, in fact, farther along their evolutionary trajectories than Capella Aa (and the β Cet type Hyads), then the possibility exists for at least some type of gradual spindown during the CHeB phase, itself: indeed, the decrease in chromospheric activity from the β Cet type Hyads to the β Gem type Hyads is proportionately comparable to the decline from Capella Ab to Aa. Since the fundamental properties—L_{bol} and T_{eff}—of the clump giants are comparatively stable during the CHeB phase, one would favor a wind-torquing mechanism like that thought to operate on the lower main sequence (e.g., Simon, Herbig, and Boesgaard 1985).

iii) *The Age of the Hyades*

The striking similarities—in bolometric luminosity and ultraviolet emission levels—between Capella Aa and the Hyades giants γ Tau and θ^1 Tau enhances the possibility—

based on the nearly identical space motions—that Capella and the Hyads truly are coeval. If so, the *age* of the cluster would be comparable to the well-established age of the Capella *secondary*: about 2.5–3 $\times$ 10^8 yr based on its definitive evolutionary status and reasonably well-known mass. That estimate is less than *half* the commonly used age of 7 $\times$ 10^8 yr derived from fitting theoretical isochrones to color-magnitude diagrams (see, e.g., review in Appendix of Barry *et al.* 1981). If the new estimate is correct, the Hyades would be closer in age to the Pleiades (7 $\times$ 10^7 yr) than previously supposed, and the many studies (e.g., Duncan 1981; Barry *et al.* 1981; Simon, Herbig, and Boesgaard 1985) which have used comparisons of the two (and other) clusters to gauge the declines of activity, rotation, and lithium abundance with age should be rethought. (Ironically, the oft-quoted study by Skumanich [1972] assumed a Hyades age of 4 $\times$ 10^8 yr, and thus would not be affected seriously). If the Hyades is as young as Capella, the validity of conventional techniques for dating cluster ages would be called into question. An intriguing, but certainly controversial, explanation for the discrepancy is *devolution* of stars in the mass range $\sim$2–3 $M_\odot$ (e.g., Willson, Bowen, and Struck-Marcell 1987).

b) Spectral Anomalies in the Secondary

The filtering, co-addition, and correction procedures applied to the SWP and LWP echellograms of Capella have produced the highest quality spectrum of a late-type star—Capella Ab—that has been achieved with the *IUE* to date. It is useful, then, to consider subtle aspects of the emission lines beyond the gross properties described in previous work (Ayres and Linsky 1980; Ayres, Schiffer, and Linsky 1983; Ayres 1984; Ayres, Jensen, and Engvold 1988).

i) N v *λ1238*, Si iv *λ1393*, *and* C iv *λ1548*

The high-excitation species N v (2 $\times$ 10^5 K); Si iv (6 $\times$ 10^4 K); and C iv (1 $\times$ 10^5 K) are recorded with excellent S/N in the spectrum of the secondary. N v λ1238 is found close to its rest wavelength, as is C iv λ1548. However, Si iv λ1393 exhibits a very significant *redshift of* +17 km s^{-1}, similar to that of C iv λ1550 (+18 km s^{-1}).

Redshifts of high-excitation emissions have been detected in *IUE* spectra of a few bright late-type stars (Ayres *et al.* 1983; Ayres, Jensen, and Engvold 1988), and are thought to result from gas-dynamic processes like those responsible for the *downflows* of 10^5 K plasma commonly observed over magnetic active regions on the Sun (e.g., Brueckner 1981).

Owing to the scrambling of detector nonuniformities by the multiple, shifted SWP echellograms, the difference in the velocities of C iv λ1548 and λ1550 almost certainly is not instrumental in origin. Furthermore, careful examination of the Si iv λ1393 and C iv λ1548 profiles reveals subtle asymmetries on the red wings of each emission: indeed, the peak of the C iv profile appears to be slightly redshifted with respect to the center of gravity of the line.

Thus, the lack of a perceptible redshift in C iv λ1548 compared with the other component of the doublet, and with Si iv λ1393, might simply be due to the Gaussian measurement technique, which tends to emphasize the centroid of the wings of the line, rather than the velocity of the extreme core. Alternatively, large opacity in the C iv feature, in a decelerating downflow, might induce selective absorption of the long wavelength wing, thus causing an intrinsically redshifted feature to appear more nearly at rest ("reverse P Cygni effect"). Finally, there are a number of weak Si i and Fe ii emissions that appear in the C iv region in high-resolution solar spectra: whether extraneous blends in the broad λ1548 feature of Capella Ab might mask an intrinsic redshift—or produce a spurious one in other features—cannot be established with the present *IUE* spectra.

ii) C ii *λ1335*

C ii λ1335 ($\sim$ 2 $\times$ 10^4 K) is one of the brightest emissions in the far-ultraviolet spectrum of the secondary. The feature is *redshifted* by +13 km s^{-1} (at the 7 σ level) in the frame of reference of narrow, low-excitation chromospheric emissions. However, the optically thick line core exhibits a significant "red asymmetry," which usually is taken to indicate the existence of *mass-outflow*. If interpreted as an absorption feature, the displacement is ~ -0.2 Å (~ -45 km s^{-1}) from the center of gravity of the C ii emission (or, ~ -30 km s^{-1} in the velocity frame defined by the low-excitation emissions). Because the C ii feature must be exceedingly optically thick, the overall redshift of the emission profile thus could be produced by partial absorption of the blue wing by an accelerating outflow of gas in the upper chromosphere.

It seems unlikely that the mass flow represents a stellar wind, however, because the *optically thin* intersystem lines Si iii] λ1892 and C iii] λ1908 both are significantly *redshifted*, indicating that the sense of the gas flow largely is inward in the layers only somewhat hotter (3–6 $\times$ 10^4 K) than those in which C ii forms. Indeed, the 6 cm radio emission from Capella barely is sufficient to explain the thermal bremsstrahlung expected from the X-ray emitting *coronal* gas in the system (Drake and Linsky 1986), let alone an additional component due to an ionized wind of significant mass-loss rate. Furthermore, the O i triplet and the Mg ii doublet show no clear signs for chromospheric mass outflow, although the emission centroids of O i λ1304 and λ1306 are redshifted by +6 km s^{-1}, almost half of the displacement exhibited by C ii λ1335. (By way of comparison, the blue-wing absorption in the O i lines of α Boo, caused by a chromospheric wind of mass-loss rate $\lesssim 10^{-10}$ $M_\odot$ yr^{-1} [Drake 1985], produces an apparent redshift of these optically thick lines of about +15 km s^{-1}; as well as virtual elimination of the shortward edges of the Mg ii *h* and *k* emission cores [see, e.g., Ayres *et al.* 1986].)

More likely, the outflow in C ii represents the low-temperature leg of a *circulation* system that feeds mass to the *corona* where it is heated to more than 10^6 K. Subsequently the gas cools and flows back to the chromosphere; on the return leg, it is visible primarily in *transition-zone* species (0.6–3 $\times$ 10^5 K), owing to the efficiency of the plasma cooling in that temperature regime. Pneuman and Kopp (1978) have proposed such a scenario to explain the existence of redshifts in *solar* transition-zone emission lines.

iii) Cl i *λ1351*

A curious spectroscopic difference between the primary and secondary is seen in Cl i λ1351: it is quite weak compared with O i] λ1355 in the spectrum of the primary, but the two emissions are about equally strong in the spectrum of the secondary (see Fig. 1*a*). Shine (1983) has proposed that the *solar* Cl i resonance line is radiatively excited by C ii λ1335 through a fluorescence mechanism. The dichotomy in $f_{\rm Cl\,I}/f_{\rm O\,I}$ between Capella Aa and Ab mirrors a similar dichotomy between C ii λ1335 and the O i triplet: $f_{\rm C\,II} \ll f_{\rm O\,I}$ in the primary, while $f_{\rm C\,II} \approx f_{\rm O\,I}$ in the secondary. These comparisons support Shine's proposal for fluorescent excitation of the Cl i line.

V. FUTURE RESEARCH

The technique I have presented for dissecting the activity levels of the components of a spectroscopic binary—modeling the residuals in differences of emission spectra taken at radial velocity extrema—is a general one; whose present applicability is limited owing to the lack of sensitivity of the *IUE* and the low resolving power of its echelles. These objections should be removed in future generations of space observatories, and thus permit the technique to be applied to a wide variety of spectroscopic binaries.

Concerning Capella itself, the precise evolutionary status of the primary is a key element in the study of the precipitous decline of stellar activity in, and beyond, the Hertzsprung gap. Some of the existing evidence points to early core-helium-burning status for Capella Aa; other evidence suggests that the primary is midway through the "clump" phase. In principle, high-precision optical and near-infrared radial-velocity spectroscopy in the spirit of the work by Shen *et al.* (1985), Fekel, Moffett, and Henry (1986), and Griffin and Griffin (1986) should provide a definitive mass ratio for the system, perhaps using the absorption analog of the emission line differencing technique to isolate the broad, shallow lines of the secondary spectrum.

Indeed, studies of Capella hardly have been exhausted: just as the *Sun* continues to reveal new, unanticipated phenomena, so too will Capella—and other bright stars—particularly as the capabilities to observe distant suns become more nearly comparable to those routinely applied to our nearby star.

I thank the staff of the NASA *IUE* Observatory, at the Goddard Space Flight Center, for their assistance in acquiring the stellar spectra; and the staff of the Regional Data Analysis Facility in Boulder, operated under contract NAS5-28731, for their help in reducing these data. Support was provided by the National Aeronautics and Space Administration through grants NAG5-199 and NGL-06-003-057 to the University of Colorado.

REFERENCES

Ake, T. B. 1982, *NASA IUE Newsletter No. 19*, p. 37.
Ayres, T. R. 1984, *Ap. J.*, **284**, 784.
———. 1985, *Ap. J. (Letters)*, **291**, L7.
Ayres, T. R., Jensen, E., and Engvold, O. 1988, *Ap. J. Suppl.*, **66**, 51.
Ayres, T. R., Judge, P., Jordan, C., Brown, A., and Linsky, J. L. 1986, *Ap. J.*, **311**, 947.
Ayres, T. R., and Linsky, J. L. 1980, *Ap. J.*, **241**, 279.
Ayres, T. R., Linsky, J. L., Vaiana, G. S., Golub, L., and Rosner, R. 1981, *Ap. J.*, **250**, 293.
Ayres, T. R., Marstad, N. C., and Linsky, J. L. 1981, *Ap. J.*, **247**, 545.
Ayres, T. R., Schiffer, F. H., III., and Linsky, J. L. 1983, *Ap. J.*, **272**, 223.
Ayres, T. R., Stencel, R. E., Linsky, J. L., Simon, T., Jordan, C., Brown, A., and Engvold, O. 1983, *Ap. J.*, **274**, 801.
Ayres, T. R., and Testerman, L. 1981, *Ap. J.*, **245**, 1124.
Baliunas, S. L., Hartmann, L., and Dupree, A. K. 1983, *Ap. J.*, **271**, 672 (BHD).
Barry, D. C., Cromwell, R. H., Hege, K., and Schoolman, S. A. 1981, *Ap. J.*, **247**, 210.
Batten, A. H., Fletcher, J. M., and Mann, P. J. 1978, *Pub. Dom. Ap. Obs.*, **15**, 121.
Bennett, J. O. 1987, Ph. D. thesis, University of Colorado.
Boesgaard, A. M. 1971, *Ap. J.*, **167**, 511.
Bohlin, R. C., and Holm, A. V. 1980, *NASA IUE Newsletter No. 10*, p. 37.
Brueckner, G. E. 1981, in *Solar Active Regions*, ed. F. Q. Orrall (Boulder: Colorado Associated University Press), p. 113.
Cash, W., Bowyer, S., Charles, P., Lampton, M., Garmire, G., and Riegler, G. 1978, *Ap. J. (Letters)*, **223**, L21.
Cassatella, A., Ponz, D., and Selvelli, P. L. 1983, *NASA IUE Newsletter* No. 21, p. 46.
Drake, S. A. 1985, in *Mass Loss from Red Giant Stars*, ed. J. E. Beckman and L. Crivellari (Boston: Reidel), p. 187.
Drake, S. A., and Linsky, J. L. 1986, *A.J.*, **91**, 3.
Duncan, D. K. 1981, *Ap. J.*, **248**, 651.
Dupree, A. K. 1975, *Ap. J. (Letters)*, **200**, L27.
Durney, B. R. 1972, in *Proc. First Solar Wind Conf.*, ed. C. P. Sonnett, P. J. Coleman, Jr., and J. M. Wilcox (NASA SP-308), p. 282.
Eggen, O. J. 1960, *M.N.R.A.S.*, **120**, 540.
Eriksson, K., Saxner, M., Gustafsson, G., Ayres, T. R., Linsky, J. L., and Andersen, J. 1986, in *New Insights in Astrophysics: Eight Years of UV Astronomy with IUE*, ed. E. Rolfe (ESA SP-263), p. 225.
Fekel, F. C., Moffett, T. J., and Henry, G. W. 1986, *Ap. J. Suppl.*, **60**, 551.
Gray, D. F. 1982, *Ap. J.*, **262**, 682.
Gray, D. F., and Endal, A. S. 1982, *Ap. J.*, **254**, 162.
Griffin, R., and Griffin, R. 1986, *J. Ap. Astr.*, **7**, 45.
Heintz, W. D. 1975, *Ap. J.*, **195**, 411.
Hoffleit, D., and Jaschek, C. 1982, *The Bright Star Catalog* (4th ed.; New Haven: Yale University Observatory).
Holm, A. V., Bohlin, R. C., Cassatella, A., Ponz, D., and Schiffer, F. H., III. 1982, *Astr. Ap.*, **112**, 34.
Iben, I., Jr. 1965, *Ap. J.*, **142**, 1447.
Johnson, H. L. 1966, *Ann. Rev. Astr. Ap.*, **4**, 193.
Kelly, R. L. 1982, "Atomic and Ionic Spectrum Lines Below 2000 Å: H through Ar" (ORNL-5922).
Kraft, R. P. 1967, *Ap. J.*, **150**, 551.
Lambert, D. L. 1981, in *Physical Processes in Red Giants*, ed. I. Iben, Jr., and A. Renzini (Dordrecht: Reidel), p. 115.
———. 1987, *Ap. J. Suppl.*, **65**, 255.
Lattanzio, J. C. 1986, *Ap. J.*, **311**, 708.
Mewe, R., *et al.* 1982, *Ap. J.*, **260**, 233.
O'Brien, G. T., Jr., and Lambert, D. L. 1986, *Ap. J. Suppl.*, **62**, 899.
Parker, E. N. 1970, *Ann. Rev. Astr. Ap.*, **8**, 1.
Pneuman, G. W., and Kopp, R. A. 1978, *Solar Phys.*, **57**, 49.
Schiffer, F. H., III. 1982, "Data Analysis Procedures for the International Ultraviolet Explorer Regional Data Analysis Facilities" (Computer Sciences Corp. TM-82/6207).
Shen, L.-Z., Beavers, W. I., Eitter, J. J., and Salzer, J. J. 1985, *A.J.*, **90**, 1503.
Shine, R. A. 1983, *Ap. J.*, **266**, 822.
Simon, T. 1984, *Ap. J.*, **279**, 738.
Simon, T., Herbig, G. H., and Boesgaard, A. M. 1985, *Ap. J.*, **293**, 551.
Skumanich, A. 1972, *Ap. J.*, **171**, 565.
Tomkin, J., Luck, R. E., and Lambert, D. L. 1976, *Ap. J.*, **210**, 694.
Vitz, R. C., Weiser, H., Moos, H. W., Weinstein, A., and Warden, E. S. 1976, *Ap. J. (Letters)*, **205**, L35.
Wallerstein, G. 1966, *Ap. J.*, **143**, 823.
Willson, L. A., Bowen, G. H., and Struck-Marcell, C. 1987, *Comm. Ap.*, **12**, 17.
Wilson, O. C. 1966, *Science*, **151**, 1487.
Wright, K. O. 1954, *Ap. J.*, **119**, 471.

THOMAS R. AYRES: Center for Astrophysics and Space Astronomy, University of Colorado, Campus Box 391, Boulder, CO 80309-0391